Monte Carlo study of the quantum spin-$\frac{1}{2}$ Heisenberg antiferromagnet on the square lattice

G. Gomez-Santos, J. D. Joannopoulos, and J. W. Negele
Department of Physics, Massachusetts Institute of Technology, Cambridge, Massachusetts 02139
(Received 29 August 1988)

A new Monte Carlo sampling technique is used to study the spin-$\frac{1}{2}$ Heisenberg antiferromagnet on square lattices of up to 256 spins. The energy, specific heat, uniform and staggered susceptibilities, and correlation function are calculated. The correlation length as a function of temperature is deduced from correlation functions and is shown to be consistent with a quantum-renormalized classical approximation. Using the coupling constant provided by Raman scattering experiments, good agreement is found between the calculated and experimental correlation lengths in La_2CuO_4.

I. INTRODUCTION

Following the discovery of high-T_c superconductors,[1] great effort has been devoted to understanding their magnetic properties. This has been motivated by the possibility of an intimate connection between magnetic behavior and the mechanism for the new superconductivity.[2–4] Neutron scattering experiments[5–7] on the prototype compound La_2CuO_4 have indeed revealed a rich magnetic structure. In particular, over a substantial range of temperatures, very strong antiferromagnet correlations in the Cu-O planes have been observed with large correlation lengths[6] but no long-range order. These features are considered to be well modeled by a quantum spin-$\frac{1}{2}$ Heisenberg antiferromagnet on a planar square lattice.

Aside from its significance for high-T_c superconductivity, the spin-$\frac{1}{2}$ Heisenberg antiferromagnet is an interesting theoretical model in its own right. Quantum fluctuations are believed to play an important role but it is not clear how they might affect the behavior one would naively expect from the classical version of the model. Even the existence of long-range order in the ground state, suggested by spin-wave treatments,[8] has been controversial.[9] Ground-state properties have been investigated using a variety of methods, including variational[9–11] and Monte Carlo[12,13] techniques, spin-wave analysis,[14] and finite-lattice calculations.[15] Finite-temperature properties, like the correlation length, have been addressed with Monte Carlo simulations[16] and renormalization-group analysis.[17]

In this paper, we study the Heisenberg antiferromagnet at finite temperature using a modification of the Handscomb Monte Carlo scheme previously considered by Lee *et al.*[18] An important new development is the introduction of a sampling procedure that more efficiently explores the configuration space. Our results show distinct differences with the recent Monte Carlo simulation of Manousakis and Salvador.[16] In particular, our calculated correlation length is generally consistent with a quantum-renormalized classical picture as advocated by Chakravarty *et al.*[17] and inconsistent with a topological-defect-driven phase transition as suggested in Ref. 16.

The paper is organized as follows. In Sec. II Handscomb's scheme is reviewed, the new sampling technique is explained, and calculations of some typical observables are presented. In Sec. III correlation functions are calculated, correlation lengths deduced, and a finite-size scaling analysis of the staggered susceptibility is performed. Finally, in Sec. IV, the extrapolated correlation length is compared with neutron scattering data, and in Sec. V we summarize the results of the paper.

II. THEORETICAL METHOD

A. Monte Carlo technique

We begin by reviewing the application of Handscomb's scheme[19] to the spin-$\frac{1}{2}$ Heisenberg antiferromagnet

$$H = J \sum_{\langle ij \rangle} \mathbf{s}_i \cdot \mathbf{s}_j \ , \tag{1}$$

where the sum is restricted to nearest-neighbor sites on a square lattice. After a trivial shift in energy, the Hamiltonian can be written as follows:[18]

$$\beta H' = \beta' \sum_{\langle ij \rangle} (h_{ij} - h_{ij}^2) \ , \tag{2}$$

where $\beta' = \beta J/2$, $\beta^{-1} \equiv T$ is the temperature multiplied by Boltzmann's constant, and the operator $h_{ij} = (S_i^+ S_j^- + S_i^- S_j^+)$ has the following action on the nearest-neighbor bond $\langle ij \rangle$:

$$h_{ij} \begin{cases} \uparrow\downarrow = \downarrow\uparrow \\ \downarrow\uparrow = \uparrow\downarrow \\ \uparrow\uparrow = 0 \\ \downarrow\downarrow = 0 \end{cases} . \tag{3}$$

After expansion of the exponential, the partition function Z' for H' can be written as[18]

$$Z' = \sum_{n=0}^{\infty} \frac{(\beta')^n}{n!} \sum_{Sn} \mathrm{Tr}(Om_1 \cdots Om_n) \ , \tag{4}$$

where Om_i stands for h_{ij} or h_{ij}^2, and the summation runs over all possible arrangements of the operators h_{ij} and h_{ij}^2 with arbitrary length (n). In (4), the bipartite nature of

 ©1989 The American Physical Society

the square lattice has been used to eliminate all minus signs. Handscomb's method considers the sum in (4) as an average over the ensemble generated by all possible strings S of both types of operators with a weight $\Pi(s)$ given by

$$\Pi(s)=\frac{(\beta')^n}{n!}\mathrm{Tr}(s) \ . \tag{5}$$

Note that the weight of a string may vanish for one of two reasons. First, because the h_{ij} operators interchange spins, they must necessarily form a closed path to produce a nonvanishing trace. Second, even if a string satisfies the previous geometrical constraint, its trace can be zero due to the order of operators and the lack of commutability of the xy and z parts of the Hamiltonian. For example, $\mathrm{Tr}h_{23}h_{12}h_{23}h_{12}=0$, whereas $\mathrm{Tr}h_{12}h_{23}h_{23}h_{12}=2$. To obtain the trace of an allowed configuration, it is convenient to introduce the notion of a cluster. A cluster is defined as the set of all sites connected by operators of the string, with the convention that each isolated site with no operators is also a cluster. Once a single spin in a cluster is specified to be up or down, the values of all other spins yielding a nonzero contribution to the trace are uniquely determined, so the trace is given by 2^{n_c}, where n_c is the number of clusters.

With the notation that $\langle\ \rangle$ denotes a statistical average with the weight (5), the energy (E), specific heat (C), uniform susceptibility (χ), antiferromagnetic structure factor [$S(\mathbf{k}=(\pi,\pi))$], and staggered susceptibility (χ_s) are given by the following averages:[18,19]

$$\begin{aligned}
E&=-\frac{\langle n\rangle}{\beta}+\frac{N_b}{4}J \ , \\
C&=\langle n^2\rangle-\langle n\rangle^2-\langle n\rangle \ , \\
\chi&=\frac{\beta}{N}\left\langle\left[\sum_i 2S_i^z\right]^2\right\rangle=\frac{\beta}{N}\left\langle\sum_\alpha (m_\alpha)^2\right\rangle \ , \\
S(\mathbf{k}=(\pi,\pi))&\equiv\frac{1}{N}\left\langle\left[\sum_i e^{i\mathbf{k}\cdot\mathbf{r}_i}2S_i^z\right]^2\right\rangle \\
&=\frac{1}{N}\left\langle\sum_\alpha (m'_\alpha)^2\right\rangle \ , \\
\chi_s&\equiv\beta S(\mathbf{k}=(\pi,\pi)) \ ,
\end{aligned} \tag{6}$$

where N is the number of sites, N_b the number of bonds, and $m_\alpha(m'_\alpha)$ represents the ferro-(antiferro-)magnetic moment of cluster α of the particular string under consideration. These moments are defined as follows:

$$\begin{aligned}
m_\alpha&\equiv\sum_{i\in\alpha}\mathrm{sgn}(i) \ , \\
m'_\alpha&\equiv\sum_{i\in\alpha}e^{i\mathbf{k}\cdot\mathbf{r}_i}\mathrm{sgn}(i), \quad \mathbf{k}=(\pi,\pi) \ ,
\end{aligned} \tag{7}$$

where the sums run over all sites of cluster α and $\mathrm{sgn}(i)$ stands for the sign $(+,-)$ of the spin at site i before it is modified by the action of the string. Note that χ_s as defined in (6) is not the cannonical staggered susceptability but rather the form useful for finite-size scaling.

B. Sampling scheme and simple test

Having specified ensemble and averages, the Monte Carlo method produces a Markov chain whose limiting distribution is given by (5). In previous applications,[16,18] the modification of a string takes place without requiring h_{ij} operators to form closed paths. As a consequence the number of forbidden configurations attempted in a typical run is close to 90%. It is clear that such a sampling procedure spends a long time trying to search an area of phase space with no physical content. In order to overcome this problem, we have devised a sampling scheme which preserves the geometrical constraint on type h_{ij} bonds. The basic steps of this new sampling technique are summarized as follows.

Given a string of operators (S_i), the Monte Carlo random walk generates another string (S_j) by means of four distinct operations which we denote as permutation, addition, deletion, and deformation.

(A) Permutation. A new string is generated by applying a random permutation to the original S_i with probability r_p.

(B) Addition. (i) An operator h_{ij}^2 is inserted on a random bond (i,j) anywhere on the lattice, at a random position in the string S_i with probability $(1-r_p)(0.5+r_a)/2$. (ii) An operator h_{ij} is inserted twice on a random bond (i,j) anywhere on the lattice, at two random positions in the string S_i with probability $(1-r_p)(0.5-r_a)/2$.

(C) Deletion. One begins by randomly choosing an operator in the present string, with probability $(1-r_p)/2$. (i) If the selected operator is of type h_{ij}^2, it is removed. (ii) If the selected operator is of type h_{ij} and it appears more than once in the string, the selected operator and another operator randomly chosen among the repeated h_{ij}'s are removed with probability r_c.

(D) Deformation. One begins by randomly choosing an operator in the present string with probability $(1-r_p)/2$. If cases C(i) and C(ii) do not apply, a deformation is performed, as described below. In order to understand deformation, it is instructive to view the selected operator h_{ij} as the part of a closed path which is to be modified by rearrangements of operators in the vicinity of bond (i,j). The selected operator occupies a physical bond in the lattice that is shared by, at most, two plaquettes denoted R and L in the example shown in Fig. 1. The first step is to select between shared plaquettes with equal probability (R in Fig. 1). The bonds in the plaquette are numbered 1 for the selected bond, 2 for the opposite bond, and 3, 4 for the lateral bonds. The following sequence of changes is made.

(i) The selected operator is removed from the string.

(ii) If the number of h_{ij} operators corresponding to bond number 3 is odd,[20] one of them is randomly removed. The same applies to h_{ij} operators corresponding to bond number 4.

(iii) If the number of h_{ij} operators corresponding to bond number 3 is even,[20] a new h_{ij} operator for bond 3 is randomly inserted. The same applies to h_{ij} operators on bond 4.

(iv) A type h_{ij} operator corresponding to bond number

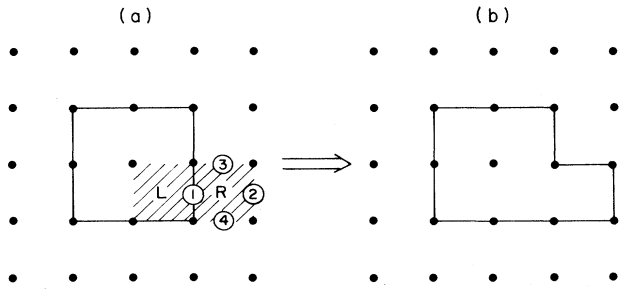

FIG. 1. Illustration of the process of deformation of a closed path (see Sec. II in text) of h_{ij} operators. (a) The selected bond (1), its two plaquettes (R and L), and the numbering of bonds in the selected plaquette (R) are shown. (b) The final configuration after "motion" of bond 1 to 2 and "creation" of bonds 3 and 4 is displayed.

2 is inserted at a random position in the string.

An example of this deformation is shown in Fig. 1, where a closed path is enlarged by moving the selected operator from bond 1 to bond 2 and generating operators at bonds 3 and 4.

For each step in the Monte Carlo process, each of these changes is performed with the specified probabilities, which were chosen to produce reasonable acceptance rates. [Of course, for the trivial case of the vacuum (zero length string) the probability of removing an operator is strictly zero and for the case of a string of length <3 we choose $r_p \equiv 0$.] Having defined a trial change in the string S_i to S_j, the new configuration is accepted or rejected depending on the value of a test ratio defined to make the Markov process microreversible.[21] Expressions for test ratios corresponding to every possible change are listed in the Appendix.

The described random walk, as complicated as it might appear, is among the simplest which preserves the geometrical constraint on h_{ij} bonds. The Markov chain so generated is reversible and satisfies the detailed balance condition. To show that all configurations can be connected by a finite number of transitions, it suffices to prove that any string can be reached from the vacuum and reduced to the vacuum. An arbitrary string can be generated as follows.

(i) Generate all h_{ij}^2 operators by addition.

(ii) Group all repeated h_{ij} operators into pairs and generate them by addition.

(iii) The remaining h_{ij} operators should form simple, nonoverlapping closed paths. These can be generated by creating suitably placed pairs of h_{ij} operators by addition and then enlarging these seeds by deformation.

(iv) Apply the necessary permutations to bring the sequence to the desired final order. Collapse of an arbitrary string to the vacuum is analogous.

The above-described scheme is able to generate all strings compatible with open boundary conditions in the square lattice. For periodic boundary conditions the method fails to produce closed paths with all possible winding numbers. Though this shortcoming is only a surface effect, it affects both types of operators in a different way, being an effective symmetry breaking term. For this reason, we have chosen to keep open boundary conditions so that the procedure remains exact.

Though the present sampling generates some configurations with zero trace due to the order in the string, its number is found to range from a few percent at high temperatures to close to 50% in the worse case at low temperatures. This should be compared with percentages as high as 95% obtained with the old sampling. In addition, because of the richer variety of moves, the new method samples the full space of string configurations more effectively and is less likely to become trapped in an unrepresentative subspace.

In order to further test the method, we have applied it to a very simple lattice for which we have exact results: a 3×2 square lattice with open boundary conditions. Because of the small size of the lattice, the comparison between the old and new schemes is not very dramatic, and for sufficiently long runs, both methods give the exact results. To show that the new method indeed searches phase space more efficiently than the old one we have chosen low temperatures and very short runs (5×10^4 steps) for which the new method is well equilibrated while the old method is not. The results are presented in Table I. All runs began with the same initial configuration (vacuum). Notice that the value of the staggered susceptibility is erroneous with the old method while consistent with the exact result for the new method. Since there are roughly half as many strings with zero trace in the new method, we have also

TABLE I. Comparison between old and new sampling schemes for a 3×2 square lattice with open boundary conditions. Energy (per site), staggered susceptibility (per site), and percentage of attempted forbidden configurations are shown for six different temperatures and Monte Carlo runs of 5×10^4 steps. Statistical errors, calculated in the standard way, are shown in parentheses.

	$T=0.04$	$T=0.05$	$T=0.075$	$T=0.1$	$T=0.15$	$T-0.25$
E (old)	−0.40 (0.03)	−0.41 (0.03)	−0.43 (0.03)	−0.47 (0.03)	−0.53 (0.02)	−0.44 (0.01)
E (new)	−0.50 (0.03)	−0.49 (0.02)	−0.52 (0.01)	−0.51 (0.01)	−0.55 (0.02)	−0.51 (0.01)
E (exact)	−0.52	−0.52	−0.52	−0.52	−0.52	−0.50
χ_s (old)	106.0 (18.0)	13.8 (0.4)	36.1 (9.0)	25.2 (7.0)	16.0 (4.0)	13.14 (0.32)
χ_s (new)	73.0 (18.0)	73.6 (8.0)	44.6 (7.0)	31.0 (3.5)	19.2 (1.5)	12.38 (0.25)
χ_s (exact)	78.0	62.46	41.6	31.2	20.7	12.28
% Forbidden conf. (old)	88	89	88	87	88	86
% Forbidden conf. (new)	46	46	44	42	41	40

effectively doubled our statistics. The reduction in the number of forbidden strings is more dramatic for larger lattices. Statistical errors (in parentheses), calculated in the standard way, are not reliable because of the highly correlated nature of these short runs.

C. Thermodynamic observables

We have performed calculations of energy, specific heat, and susceptibilities on three different lattice sizes, 8×8, 12×12, and 16×16, with open boundary conditions. We begin our discussion with some general considerations. Lengths of typical runs vary from 2 million steps for high temperatures to, at most, 16 million steps for low temperatures. Error bars were obtained in the standard way by dividing the entire run into bins (~10) and measuring the statistical dispersion of bin averages.

In the Handscomb method, the length of the string grows linearly with inverse temperature at slow temperatures, irrespective of lattice size. This behavior poses a major problem in reaching low temperatures. This is especially true for the staggered susceptibility which exhibits wild fluctuations and slow dynamics at low temperatures. For this reason, results for the susceptibilities are restricted to temperatures above 0.375, 0.375, and 0.40 for lattice sizes 8×8, 12×12, and 16×16, respectively.

A very important aspect of the Heisenberg Hamiltonian is its rotational invariance, which should be preserved by the Monte Carlo simulation. The limiting distribution of the described Markov chain should indeed be isotropic. However, since the Handscomb scheme inherently treats the xy and z components of the Hamiltonian in a different fashion, it is important to have a measure of this isotropy. The abstract nature of the phase space in Handscomb's method makes it impractical to perform a rigorous check of the isotropy of the simulation. However, one reasonable criterion is to require that the nearest-neighbor zz correlation $\langle S_i^z S_j^z \rangle$ agree with the value obtained from the energy (6) assuming perfect isotropy. This isotropy criterion is satisfied, within error bars, for all data shown in this paper and has guided us in deciding the lowest acceptable temperature for every lattice size.

In Figs. 2–4 we show the results of our calculation for the energy, specific heat, and susceptibilities. Error bars are displayed for the largest lattice size shown. Note that the energy and specific heat are normalized to the number of bonds, which corrects a large part of the finite-size effects intrinsic to open boundary conditions. The specific heat has been calculated from the energy data for the 12×12 lattice. Use of expression (6) gives equivalent results but with poorer statistical quality. No significant lattice size dependence can be observed in the specific heat.

The uniform susceptibility shows smooth behavior with a shallow maximum, as expected, while the antiferromagnetic structure factor displays significant growth with decreasing temperature and noticeable lattice size dependence. Results of available[22–24] high-temperature series expansions (HTSE), plotted as continuous lines in Figs. 2–4, show good agreement with our data in the appropriate temperature regime.

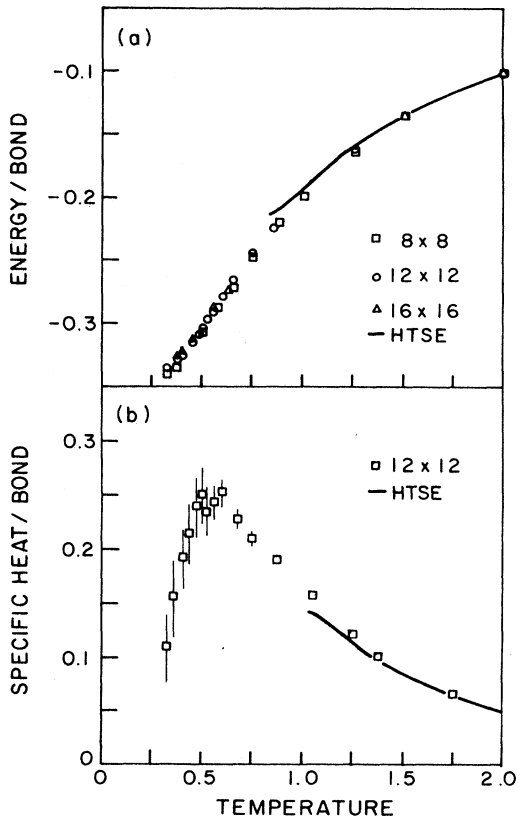

FIG. 2. (a) Energy per bond vs temperature in units of J with results of high-temperature series expansion (HTSE). (b) Specific heat per bond (in units of k_B) obtained from numerical differentiation of energy data for the 12×12 lattice and high-temperature series expansion (HTSE).

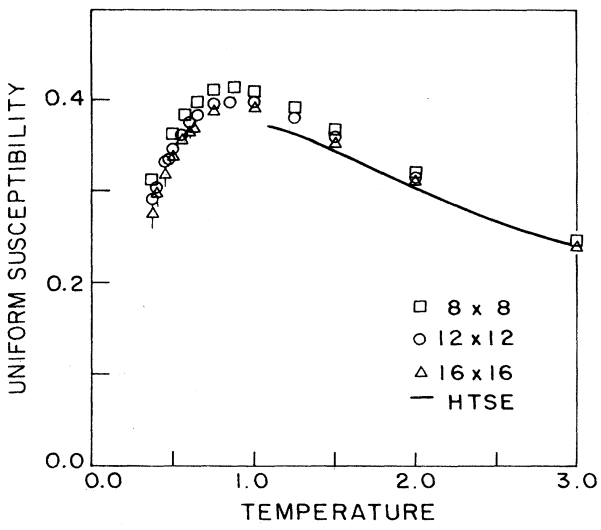

FIG. 3. Uniform susceptibility vs temperature (in units of J) with results of high-temperature series expansion (HTSE).

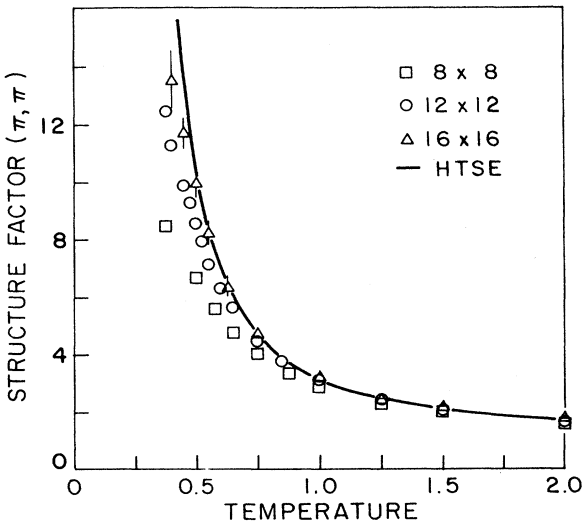

FIG. 4. Antiferromagnetic structure factor vs temperature (in units of J) with results of high-temperature series expansion (HTSE).

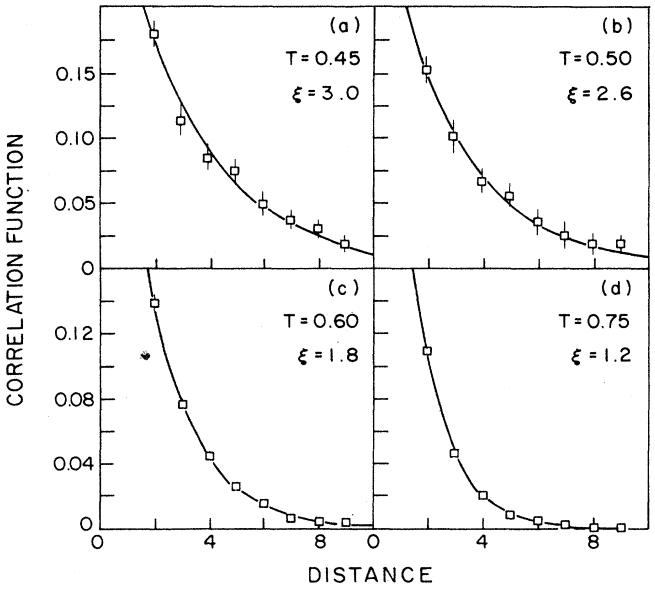

FIG. 5. Absolute value of the zz pair correlation function for four representative temperatures of the 16×16 lattice. Continuous lines are fits to pure exponentials [$\propto \exp(-r/\xi)$].

III. CORRELATION LENGTH AND FINITE-SIZE SCALING

A. Correlation length

In order to get information about the correlation length we have calculated the zz pair correlation function $C(i,j)$

$$C(i,j)=4\langle s_i^z s_j^z\rangle \ . \tag{8}$$

The value of $C(i,j)$ for a given string of operators in our statistical ensemble is given by

$$C(i,j)=\begin{cases}\mathrm{sgn}(i)\mathrm{sgn}(j), & \text{if } i,j\in \text{ same cluster}\\ 0, & \text{otherwise}\end{cases} \tag{9}$$

with $\mathrm{sgn}(i)$ defined as in Sec. II A.

Because of the lack of translational invariance imposed by our boundary conditions, we have calculated correlation functions for equivalent pairs along the two central columns and rows of our lattices. For a given separation, we have selected all the equivalent pairs of points whose midpoint lies closest to the lattice center.

Typical results are shown in Fig. 5 for the 16×16 lattice. Correlation lengths ξ have been obtained by fitting selected data with $Ce^{-r/\xi}$. The nearest-neighbor correlation has been removed in all cases and fits have been restricted to distances less than half the lattice size, to reduce surface effects. These fits are found to be very satisfactory with quality never worse than that shown in Fig. 5.

The correlation length as a function of temperature, for different sizes, is plotted in Fig. 6. Manousakis and Salvador[16] have recently performed similar calculations for the correlation length. The result of their fit to a Kosterlitz-Thouless[25] form for the correlation length, $C\exp(D/\sqrt{T-T_c})$, is shown as a dashed line in Fig. 6. While general agreement between both calculations is found at high temperature, our correlation length increases slower with decreasing temperature than that of Ref. 16. Although error bars are large at low temperatures, we believe that the difference between both calculations is systematic and cannot be attributed to statistical

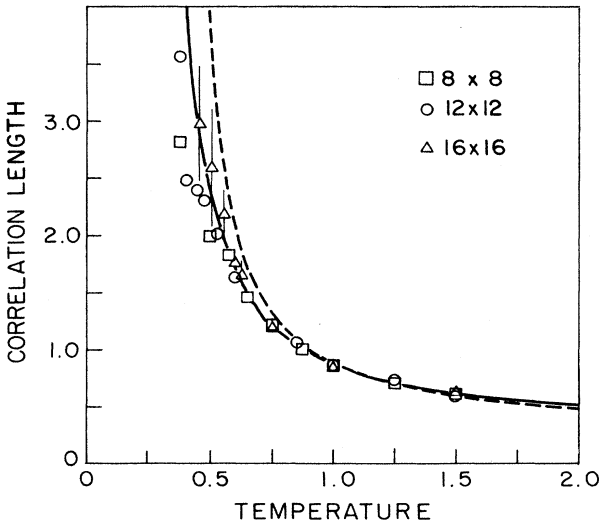

FIG. 6. Correlation length in units of lattice constant vs temperature in units of J. Error bars are only shown for the largest size. The solid line is the best fit of the data to $A\exp(2\pi Js^2B/T)$ with $A=0.32$ and $B=0.635$. The dashed line represents the results of Ref. 14, which used a fit to $C\exp(D/\sqrt{T-T_c})$ with $C=0.178$, $D=1.338$, and $T_c=0.3$.

dispersion. The most probable origin of the discrepancy is the fact that the new sampling method described in this work searches phase space more efficiently than the method of Ref. 16.

The classical analog of the Heisenberg antiferromagnet is believed to have a correlation length which diverges exponentially at zero temperature[26–29]

$$\xi \sim \exp(2\pi J s^2/T) . \tag{10}$$

A recent renormalization-group study of an extended nonlinear σ model[17] indicates that the classical picture remains valid in the quantum antiferromagnetic case with parameters renormalized by quantum fluctuations. To two-loop order, the following form for the correlation length is suggested:

$$\xi = A \exp(2\pi J s^2 B/T) . \tag{11}$$

We have fitted this expression to our data for ξ and obtain a good fit with $A=0.32$ and $B=0.635$, as illustrated by the solid line in Fig. 6. We note that B can be considered as the quantum renormalization of the coupling constant, and its value is consistent with results of the renormalization-group study, which yield[30] $B \sim 0.6-0.7$. Thus, in contrast to the work of Manousakis and Salvador,[16] we do not need to invoke the presence of a Kosterlitz-Thouless phase transition to explain the behavior of the correlation length. To investigate this point further, we perform a finite-size scaling analysis in the next subsection.

B. Finite-size scaling

In what follows, we analyze finite-size effects in the staggered susceptibility (Fig. 4) using the information obtained for the correlation length. A renormalization-group study of the nonlinear σ model gives the following scaling form for the Fourier transform of the pair correlation function:[31]

$$G(\mathbf{p},T)=[\xi(T)]^2[\sigma(T)]^2 F(\mathbf{p}\xi) , \tag{12}$$

where $\mathbf{p}$ is the reciprocal space vector, F is an arbitrary function, and $[\sigma(T)]^2 \propto T^2$ at low temperatures. This expression suggests a finite-size scaling for the staggered susceptibility of the form

$$\frac{\chi_s}{L^2 T} = f(\xi/L) , \tag{13}$$

where L is the lattice size and $f(\xi/L)$ an unknown function.

It is important to keep in mind that finite-size scaling assumes that we are close to the critical region ($\xi \gg a$), so it is essential that the scaling collapses all the data onto a single curve at the largest correlation lengths. In Fig. 7(a) we show χ_s/T versus ξ given by expression (11) with our values of A and B for the three lattice sizes. The effects of finite-size scaling are illustrated in Fig. 7(b). The data clearly tend to collapse nicely along a single curve especially at large correlation lengths.

In an attempt to test if a Kosterlitz-Thouless expression could be consistent with our results, we have fitted

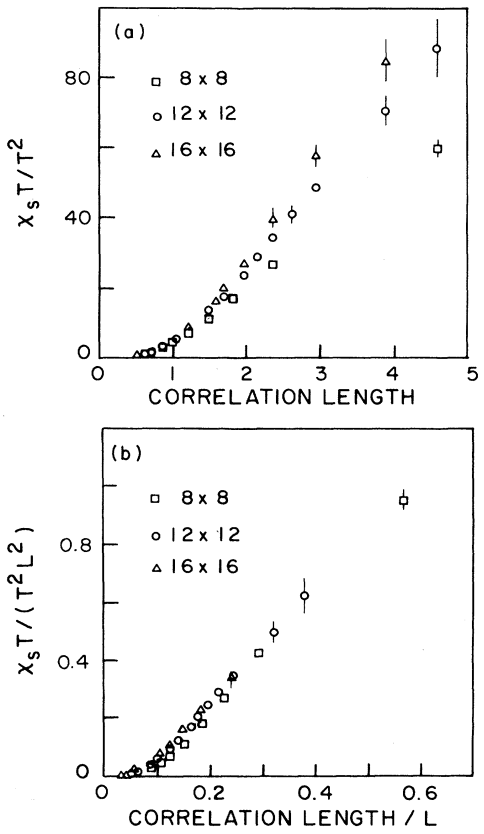

FIG. 7. Finite-size scaling analysis of the staggered susceptibility according to expression (13) in the text, using the best fit of ξ to $A \exp(2\pi J s^2 B/T)$. (a) Unscaled data. (b) Scaled data.

our calculated correlation length on a (16×16) lattice to a Kosterlitz-Thouless form $\xi = C \exp[D/(T-T_c)^{1/2}]$. The best fit to our data is obtained with $C=0.11$, $D=2.14$, and $T_c \simeq 0$. The corresponding finite-size scaling dictated by a Kosterlitz-Thouless transition with exponent $\eta=\frac{1}{4}$ is given by

$$\frac{\chi_s T}{L^{2-\eta}} = f(\xi/L) . \tag{14}$$

In Figs. 8(a) and 8(b) we show the unscaled and scaled curves corresponding to this expression. Unlike the situation displayed in Figs. 7(a) and 7(b), the scaled curves of Fig. 8(b) run parallel to each other with no clear tendency toward merging for large ξ (compare, for instance, the behavior of the 8×8 and 12×12 lattices in both cases).

In summary, we believe that our data for the correlation length at $T>0.375$ are consistent with a quantum-renormalized classical picture[17] and no indication of topological-defect phase transition is found.

IV. EXPERIMENTAL IMPLICATIONS

As mentioned in the Introduction, magnetic properties of La_2CuO_4 have been studied by means of neutron

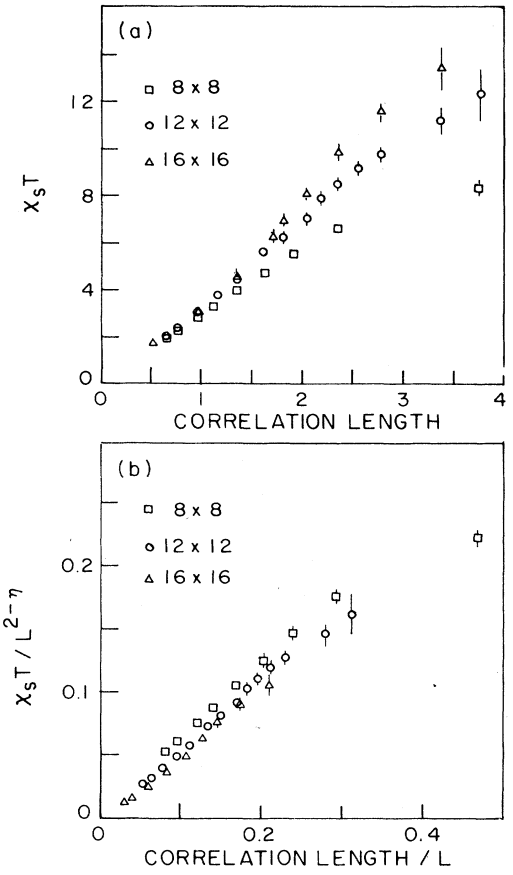

FIG. 8. Finite-size scaling analysis of the staggered susceptibility according to expression (14) in the text, with ξ given by the best fit of our data to $C\exp(D/\sqrt{T-T_c})$. (a) Unscaled data. (b) Scaled data.

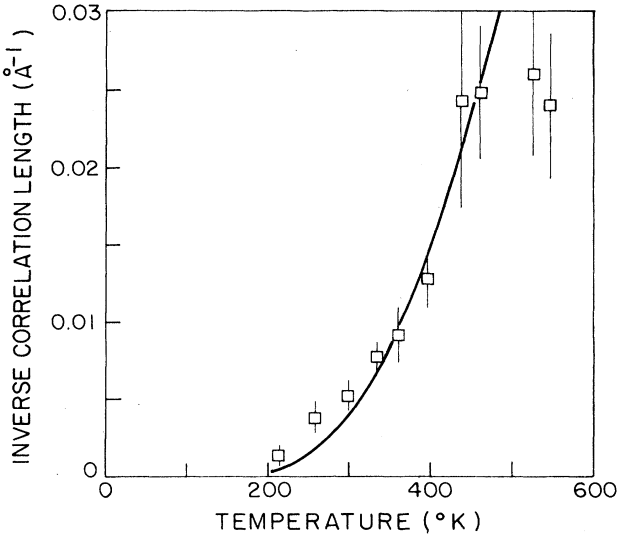

FIG. 9. Inverse correlation length vs temperature. Open squares are results of neutron scattering experiments on La_2CuO_4. The continuous line represents our theoretical result Eq. (15) using the experimental values $a_0=3.78$ Å and $J=1600$ K.

scattering.[5–7] In particular, the correlation length has been obtained as a function of temperature,[6] and in this section we analyze these data in the context of our Monte Carlo results.

A direct comparison between experiment and our Monte Carlo data is not possible because the measured correlation length is much longer than that accessible from the Monte Carlo calculation. However, having determined the parameters of the quantum corrected renormalization-group correlation length to be

$$\xi=0.32a_0\exp(2\pi Js^2 0.635/T)\ , \tag{15}$$

and having verified that this functional form has a scaling behavior that appears to be correct, it is instructive to compare this expression with the experimental data. Using the lattice parameter $a_0=3.78$ Å corresponding to La_2CuO_4 only the coupling constant J is needed in (15) to obtain ξ. This coupling constant has been obtained from spin-pair Raman scattering[32] and the value reported is $J\sim 1600$ K (1100 cm^{-1}).

In Fig. 9 we show the experimental inverse correlation length versus temperature and compare it with the Monte Carlo fit given by (15) with the experimental values of a_0 and J. The agreement is quite satisfactory, and we conclude that our extrapolated correlation length is perfectly consistent with neutron scattering results using the experimental value of J from Raman scattering.

We close this section by noting the significance of the large energy scale of J in connection with the absence of Curie behavior of the measured uniform susceptibility in La_2CuO_4. This susceptibility shows a mild increase at high temperature instead of the usual T^{-1} Curie law.[33] The observed increase is consistent with our calculated susceptibility considering the fact that, for the experimental value of J, the maximum temperature of the experiment (800 K) corresponds to $T=0.5$ in Fig. 3. Physically, the large value of J makes the system strongly correlated even at the highest measured temperatures as opposed to the mere collection of almost independent spins required for the Curie law to apply. Although the previous statement is certainly true for a spin-$\frac{1}{2}$ Heisenberg antiferromagnet with large J, it should be kept in mind that, in the real material, other effects not modeled by our Hamiltonian might come into play.

V. SUMMARY

We have investigated finite-temperature properties of the spin-$\frac{1}{2}$ Heisenberg antiferromagnetic model in the square lattice, considered relevant for the magnetic properties of La_2CuO_4 superconductors. The model has been studied with a Monte Carlo technique based on Handscomb's scheme.

The sampling of the Handscomb method has been generalized to produce a much more thorough search of

phase space. Typical observables like the energy, specific heat, and susceptibilities have been calculated showing good statistical quality and agreement with series expansions in the appropriate limit.

Correlation functions have been calculated and from them, the correlation length has been obtained as a function of temperature. The results are consistent with a quantum renormalized classical picture, as suggested by a recent renormalization-group treatment of an extended nonlinear model.[17] Contrary to the suggestion of a similar calculation,[16] no need for a topological-defect-driven phase transition is required to explain our data.

Extrapolation of our fitted form for the correlation length to the experimental regime shows excellent agreement with neutron scattering data[6] when the experimental (Raman) value for the coupling constant[32] is used. Although we have thus demonstrated that the quantum renormalized-correlation function is consistent with both experiments at low T and Monte Carlo results at higher T, the present Monte Carlo scheme is not able to address directly the low-temperature regime corresponding to truly critical behavior.

ACKNOWLEDGMENTS

The authors would like to thank Professor M. Kardar, Professor B. I. Halperin, and E. Tarnow for helpful discussions. This work has been supported in part by the U. S. Office of Naval Research Grant No. N00014-770-C-0132 and U.S. Department of Energy (DOE) Contract No. DE-AC02-76 ER03069. One of us (G.G-S.) acknowledges additional support from the Fulbright-MEC program.

APPENDIX

In Sec. II we described all possible changes of a string of operators (S_i) in the Monte Carlo process. A modified configuration (S_j) is accepted with probability one if the test ratio (R_t) is greater than one and with probability R_t if R_t is less than one. In this Appendix we write the expressions of R_t for every elemental step of Sec. II. In what follows, symbols retain the meaning given previously unless otherwise stated.

A. Permutation

$$R_t=\frac{\mathrm{Tr}(S_j)}{\mathrm{Tr}(S_i)} .$$

B. Addition

$$\text{(i)}\quad R_t=\frac{\beta' N_b \mathrm{Tr}(S_j)}{(n+1)(0.5+r_a)\mathrm{Tr}(S_i)} ,$$

$$\text{(ii)}\quad R_t=\frac{(\beta')^2 N_b r_c \mathrm{Tr}(S_j)}{(n+2)(0.5-r_a)(n_1-1)\mathrm{Tr}(S_i)} ,$$

where n is the length of S_i and n_1 is the number of type-h_{ij} operators equal to the added ones in the final string S_j.

C. Deletion

$$\text{(i)}\quad R_t=\frac{n(0.5+r_a)\mathrm{Tr}(S_j)}{\beta' N_b \mathrm{Tr}(S_i)} ,$$

$$\text{(ii)}\quad R_t=\frac{n(0.5-r_a)(n_1+1)\mathrm{Tr}(S_j)}{(\beta')^2 N_b r_c \mathrm{Tr}(S_i)} ,$$

where n is the length of S_i and n_1 is the number of type-h_{ij} operators equal to the removed ones in the final string S_j.

D. Deformation

$$R_t=\frac{n_{p1} n (\beta')^{n'-n}\mathrm{Tr}(S_j) A(n_3,n_4) B(n_1,n_2)}{n_{p2} n' \mathrm{Tr}(S_i)} ,$$

where $n(n')$ is the length of $S_i(S_j)$, $n_{p1}(n_{p2})$ is the number of plaquettes sharing the bond number 1(2), and n_1, n_2, n_3, n_4 are the number of type h_{ij} operators corresponding to bond 1, 2, 3, 4, respectively, in the final string S_j. $A(n_3,n_4)$ and $B(n_1,n_2)$ are defined as

$$A(n_3,n_4)\equiv(n_3+\sigma_3)^{2\sigma_3-1}(n_4+\sigma_4)^{2\sigma_4-1}$$

with

$$\sigma_i=\begin{cases}1 & \text{if operator is removed in bond i}\\ 0 & \text{if operator is added in bond i}\end{cases}$$

and

$$B(n_1,n_2)=\begin{cases}1-r_c & \text{if } n_1=0 \text{ and } n_2>1\\ (1-r_c)^{-1} & \text{if } n_1\geq 1 \text{ and } n_2=1\\ 1 & \text{otherwise .}\end{cases}$$

In special cases,the following trivial changes are needed. (i) If after a deletion the final string is the vacuum, the test ratio should be multiplied by 2. (ii) If the original string is the vacuum, only additions are possible and the corresponding test ratios should be divided by 2. (iii) Test ratios for modifications that change S_i from $n\leq 2$ (no permutations) to $n>2$ should be multiplied by $(1-r_p)$. Test ratios should be divided by $(1-r_p)$ for the opposite case.

[1]J. G. Bednorz and K. A. Müller, Z. Phys. B **64**, 189 (1986).
[2]P. W. Anderson, Science **235**, 1196 (1987).
[3]T. M. Rice, Z. Phys. B **67**, 141 (1987), and references therein.
[4]P. W. Anderson, Phys. Rev. Lett. **59**, 2497 (1987), and references therein.
[5]G. Shirane, Y. Endoh, R. J. Birgeneau, M. A. Kastner, Y. Hidaka, M. Oda, M. Suzuki, and T. Murakami, Phys. Rev. Lett. **59**, 1613 (1987).

[6]Y. Endoh, K. Yamada, R. J. Birgeneau, D. R. Gabbe, H. P. Jenssen, M. A. Kastner, C. J. Peters, P. J. Picone, T. R. Thurston, J. M. Tranquada, G. Shirane, Y. Hidaka, M. Oda, Y. Enomoto, M. Suzuki, and T. Murakami, Phys. Rev. B **37**, 7443 (1988).

[7]D. Vaknin, S. K. Sinha, D. E. Moncton, D. C. Johnston, J. M. Newsam, C. R. Safinya, and H. E. King, Jr., Phys. Rev. Lett. **58**, 2802 (1987).

[8]P. W. Anderson, Phys. Rev. **86**, 694 (1952).

[9]S. Liang, B. Doucot, and P. W. Anderson, Phys. Rev. Lett. **61**, 365 (1988).

[10]P. Horsch and W. von der Linden (unpublished).

[11]D. A. Huse and V. Elser, Phys. Rev. Lett. **60**, 2531 (1988).

[12]J. D. Reger and A. P. Young, Phys. Rev. B **37**, 5978 (1988).

[13]T. Barnes and E. S. Swanson, Phys. Rev. B **37**, 9405 (1988).

[14]D. A. Huse, Phys. Rev. B **37**, 2380 (1988).

[15]J. Oitmaa and D. D. Betts, Can. J. Phys. **56**, 897 (1978).

[16]E. Masousakis and R. Salvador, Phys. Rev. Lett. **60**, 840 (1988).

[17]S. Chakravarty, B. I. Halperin, and D. R. Nelson, Phys. Rev. Lett. **60**, 1057 (1988).

[18]D. H. Lee, J. D. Joannopoulos, and J. W. Negele, Phys. Rev. B **30**, 1599 (1984).

[19]D. C. Handscomb, Proc. Cambridge Philos. Soc. **58**, 594 (1962); **60**, 116 (1964).

[20]The reason for distinguishing between odd and even numbers of operators is to have a simple rule for assuring reversibility of the Markov chain while, in contrast to addition and deletion, keeping the number of operators in the string as constant as possible.

[21]W. K. Hastings, Biometrika **57**, 97 (1970).

[22]G. S. Rushbrooke, G. A. Baker, Jr., and P. J. Wood, in *Phase Transitions and Critical Phenomena,* edited by C. Domb and M. G. Green (Academic, New York, 1974), Vol. 3.

[23]M. F. Collins, Phys. Rev. B **2**, 4552 (1970).

[24]G. A. Baker, Jr., H. E. Gilbert, J. Eve, and G. S. Rushbrooke, Phys. Lett. **25A**, 207 (1967).

[25]J. Kosterlitz and D. Thouless, J. Phys. C **6**, 1181 (1973); J. Kosterlitz, *ibid.* **7**, 1046 (1974).

[26]A. M. Polyakov, Phys. Lett. **59B**, 79 (1975).

[27]E. Brezin and J. Zinn-Justin, Phys. Rev. B **14**, 3110 (1976).

[28]D. R. Nelson and R. A. Pelcovits, Phys. Rev. B **16**, 2191 (1977).

[29]S. H. Shenker and J. Tobochnik, Phys. Rev. B **22**, 4462 (1980).

[30]B. I. Halperin (private communication).

[31]D. J. Amit, *Field Theory, the Renormalization Group, and Critical Phenomena* (World Scientific, Singapore, 1984).

[32]K. B. Lyons, P. A. Fleung, J. P. Remeika, A. S. Cooper, and T. J. Negran, Phys. Rev. B **37**, 2353 (1988).

[33]See, for instance, D. C. Johnston, J. P. Stokes, D. P. Goshom, and J. T. Lewandowski, Phys. Rev. B **36**, 4007 (1987).